Carboxyl-Terminated Butadiene Acrylonitrile Rubber/ Epoxy Polymer Alloys as Damping Adhesives and Energy Absorbable Resins

Hajime Kishi, Atsushi Nagao, Yusaku Kobayashi, Satoshi Matsuda, Toshihiko Asami, Atsushi Murakami

Graduate School of Engineering, Himeji Institute of Technology, University of Hyogo, 2167, Shosha, Himeji, Hyogo 671-2201, Japan

Received 27 October 2006; accepted 5 January 2007
DOI 10.1002/app.26189
Published online in Wiley InterScience (www.interscience.wiley.com).

ABSTRACT: Carboxyl-terminated butadiene acrylonitrile (CTBN) liquid rubber/epoxy (diglycidyl ether of bisphenol-A: DGEBA) / diamino diphenyl methane (DDM) resins, in which CTBN was 60 wt % as the major component, were formulated to evaluate the damping and adhesive properties. In cases where acrylonitrile (AN) was 10∼18 mol % as copolymerization ratio in CTBN, the blend resins showed micro-phase separated morphologies with rubber-rich continuous phases and epoxy-rich dispersed phases. The composite loss factors (η) for steel laminates, which consisted of two steel plates with a resin layer in between, depended highly on the environmental temperature and the resonant frequencies. On the other hand, in the case where AN was 26 mol % in CTBN, the cured resin did not show clear micro-phase separation, which means the components achieve good compatibility in nano-scale. This polymer alloy had a broad glass-transition temperature range, which resulted in the high loss factor ($\eta > 0.1$) for the steel laminates and excellent energy absorbability as the bulk resin in a broad temperature range. Also the resin indicated high adhesive strengths to aluminum substrates under both shear and peel stress modes. The high adhesive strengths of the CTBN/epoxy polymer alloy originated in the high strength and the high strain energy to failure of the bulk resin. J Appl Polym Sci 105: 1817–1824, 2007

Key words: epoxy; rubber; resins; damping; adhesives; energy absorbability

INTRODUCTION

Vibration and noise is an environmental problem. Much effort has been devoted to achieve vibration damping in many industries. As a result, the problems arising from factories have been reduced in recent years. According to statistic data,[1] however, the vibration and noise from transportation such as automotives and those from construction industries is still serious.

Adhesives are functional polymers, which are often used in automotive and construction industries. As structural adhesives, epoxy resins are often applied because of their high adhesive strength and solvent resistance. It would be desirable if one can add high damping performance to the structural adhesives. In particular, with the increase of the use of fiber reinforced composites in those industries, the role of the adhesives should also increase, because composites are not able to be welded.

Correspondence to: H. Kishi (kishi@eng.u-hyogo.ac.jp).

Journal of Applied Polymer Science, Vol. 105, 1817–1824 (2007)

In general, polymers are materials with damping performance especially at the glass-transition temperature. The molecular motion and the friction of polymer chains convert given mechanical energy into thermal energy and dissipate it as heat release.[2] Homopolymers have narrow glass-transition regions, which cause the narrow temperature range with damping performance. One way to broaden the glass-transition regions is using polymer blend.[3] Among many polymer blends, interpenetrating polymer networks (IPNs) were studied most to achieve the wide glass-transition regions,[4–6] which related to the wide range of temperature with high-damping performance. IPNs are defined as the intimate mixture of two or more crosslinked polymers in which one network is formed in the presence of another.[7] IPNs can be formed by both simultaneous polymerization[8,9] and sequential polymerization.[10,11] Ideally, interpenetration occurs only through physical crosslinks and mixing is on a molecular scale as long as no covalent bonds exist between the differing polymers.[4] Control of compatibility (morphology) and viscoelastic properties of the multi-component resin system would be the key to improve the damping performances.

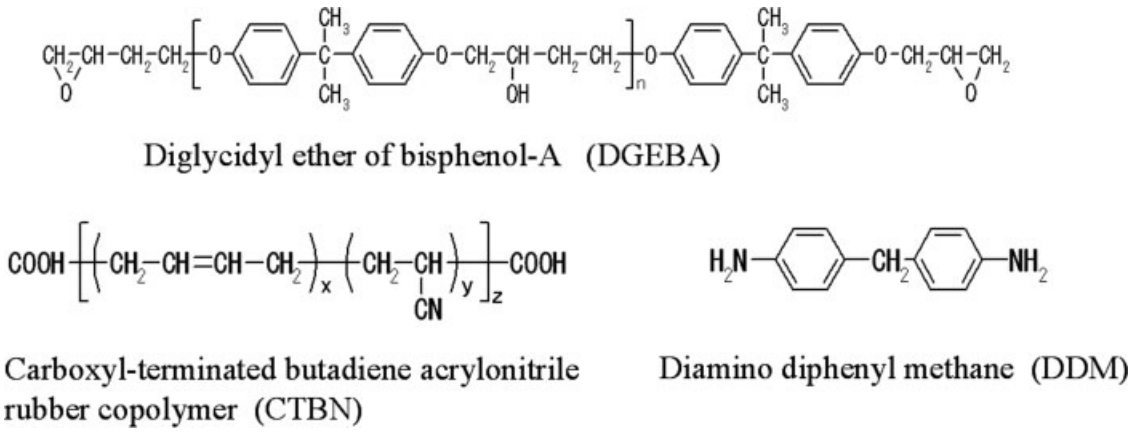

Figure 1 Chemical structure of resin components.

The main components of the resins used in this study were epoxy resins and reactive liquid rubbers. In this case, all the components (epoxy monomers, reactive rubbers, and curing agents) reacted chemically with each other and generated covalent bonded networks. Therefore, the resulting network structures are out of the definition of IPNs above-mentioned. To achieve both damping over a wide range of temperature and good adhesive properties, the objective of this study was first to find the dominant factors, which control the morphology and viscoelastic properties of the multicomponent adhesive resins. Second, the study focused on the energy absorbability of bulk resins as well as the damping performance of adhesives. Third, the adhesive properties and the mechanism were also examined. Although the combination of epoxy resins and reactive liquid rubbers is well known as the toughened epoxy systems,[12–15] one of the differences of this study, compared with others, is in the resin composition. Namely, the reactive liquid rubber was used as the major component (60 wt %) of the blends, so the control of the compatibility among the components generated new categorized epoxy polymer alloys, which possess both high damping and adhesive performances.

EXPERIMENTAL

Materials

Diglycidyl ether of bisphenol-A oligomers (DGEBA) were used as epoxy resins. The epoxy equivalents were 189 g/equiv. Three kinds of carboxyl-terminated butadiene acrylonitrile (CTBN) rubbers were used as major components in resin compositions. The number average molecular weight of CTBNs was about 3500. The acrylonitrile contents in CTBNs were 10, 18, and 26 mol %, respectively. Diamino diphenyl methane (DDM) was used as the curing agent. The chemical structures of these resin components were shown in Figure 1. Triphenyl phosphine (TPP) was used as a catalyst for the reaction between carboxyl groups in CTBNs and epoxies. The resin formulation (weight ratio) was DGEBA/CTBN/DDM = 100/172.4 (60 wt %)/14.4, compared with a conventional epoxy resin: DGEBA/DDM = 100/26.2 as a reference material.

Prereaction between CTBN and epoxy resins

DGEBA, CTBN, and TPP as a catalyst were first mixed in a glass flask at 25°C and the temperature was raised to 160°C while stirring. The flask was kept at the same temperature in 2 h for the prereaction between DGEBA and CTBN, then cooled down to room temperature. The reaction scheme between carboxyl groups in CTBN and epoxy groups in DGEBA was shown in Figure 2.

Preparation of cured resins

CTBN/epoxy prereacted resin and DDM were mixed first and heated to 100°C to lower the viscosity of the resin, making it easier to disperse the DDM particles. Then, the resin compositions were held at 100°C under a vacuum to de-gas. The resin compositions were poured into preheated silicone-coated molds and cured at 130°C for 4 h.

A conventional epoxy resin: DGEBA/DDM was used as a reference material. The resin composition was cured at 180°C for 2 h.

Evaluation of viscoelasticity of the cured resins

The temperature dependencies of the viscoelastic properties (storage modulus: E' and loss tangent: tanδ) of the cured resins were evaluated by dynamic mechanical analysis (DMA) in the tensile mode (span: 20 mm) at a dynamic frequency of 1 Hz and an amplitude of 10 μm using a DMS6100 (Seiko

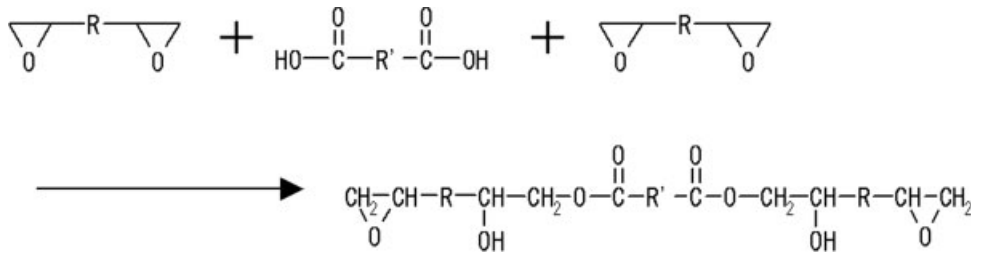

Figure 2 The reaction scheme between carboxyl groups in CTBN and epoxy groups in DGEBA.

Instruments) instrument. Cured resin specimens with a length of 40 mm, a width of 10 mm, and a thickness of 2 mm were machined from 2 mm-thick cured plaques. The samples were tested over a temperature range between −100 and 150°C with a heating rate of 2°C/min.

Scanning electron microscopy observation

Thin sections of the cured resins were stained by vapor of OsO_4 and observed using a scanning electron microscope (FE-SEM) ''JSM-6340F'' made by JEOL in reflected electron mode. The samples were mounted on brass stubs and were coated with a thin layer of platinum using an ion sputter coater. The OsO_4 stains the rubber-rich regions by depositing osmium in areas containing the unsaturated molecules,[16] i.e., the butadiene in this study. In the reflected electron mode, the OsO_4-stained regions were observed as bright areas.

Damping tests of steel laminates with the resin layer

The steel laminate beam specimens, which consisted of two steel plates with the resin layer in between, were rectangular in shape, 180 mm (in length) × 10 mm (in width). The damping property (loss factor: η) of the laminates was measured by the mechanical impedance method, in which the specimen is forced to vibrate at its center, as shown in Figure 3.

A swept sine signal was used for the excitation wave form. Both the driving force (F) transmitted to the specimen and the acceleration (A) at the excitation point were measured by a sensor called the impedance head. The ratio of the output signal (F) to the input signal (A) was analyzed by the FFT analyzer. The mechanical impedance versus frequency was recorded and the loss factor (η) was computed using the relationship as follows:

$$\eta = \triangle f/f_n \ (= \tan\delta)$$

where Δf is the bandwidth of frequency at 3 dB below from the peak amplitude, and f_n is the resonant or peak frequency.

Evaluation of adhesive strength

Shear adhesive strength

Test specimens were prepared using aluminum substrates that had been wiped with acetone to prepare the surfaces for bonding. The dimensions of the aluminum substrates were length 150 mm, width 25 mm, and thickness 1.5 mm. Adhesive resin was applied to the aluminum substrates, which were then brought into contact, and the bonded joint was cured at 130°C for 4 h. The lap joint length was 12.5 mm. The tensile shear adhesive strength of the specimens was evaluated using the test machine ''INSTRON 5582'' in accordance with JIS K 6850 at a crosshead speed of 10 mm/min at 23°C.

Peel adhesive strength

T-peel test specimens were also prepared using thin aluminum substrates. The dimensions of the aluminum substrates were length 200 mm, width 25 mm, and thickness 0.5 mm. The T-peel adhesive strength of the specimens was evaluated using the test machine ''INSTRON 5582'' in accordance with JIS K 6854-3 at a crosshead speed of 100 mm/min at 23°C.

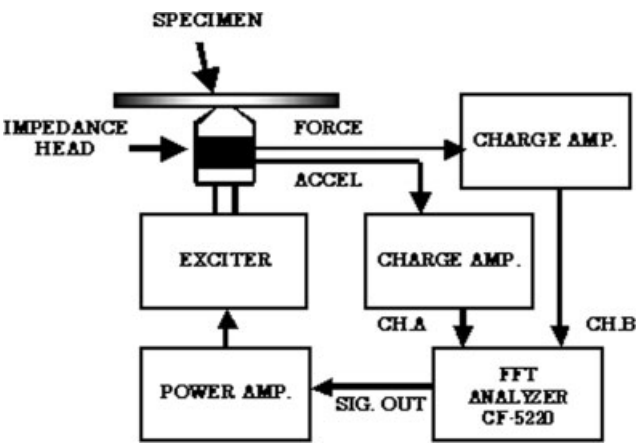

Figure 3 Measuring of the loss factor of steel laminates with resin layer in between.

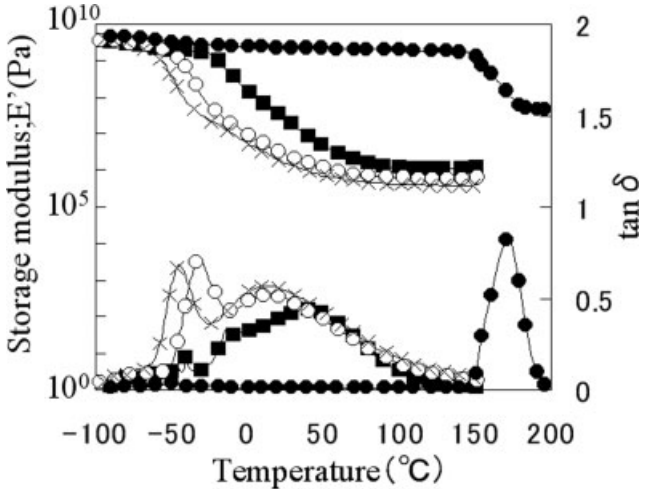

Figure 4 Dynamic viscoelastic properties of formulated epoxy resins, measured at 1 Hz: ×, DGEBA/DDM/CTBN (100/14.4/172.4), AN content: 10 mol % in CTBN; (○), DGEBA/DDM/CTBN (100/14.4/172.4), AN content: 18 mol % in CTBN; (■), DGEBA/DDM/CTBN (100/14.4/172.4), AN content: 26 mol % in CTBN; (●), DGEBA/DDM (100/26.2).

Evaluation of tensile properties of the cured resins

Tensile properties of cured resins were evaluated using JIS K 7113 at a crosshead speed of 10 mm/min using the specimen in dog-bone shape. The dimensions of specimens were span length 30 mm, width 5 mm, and thickness 2 mm.

Evaluation of energy absorbability of cured resin laminates

Energy absorbability of cured resin laminates were evaluated using a Schob pendulum type impactor. A 200-g pendulum was dropped from 250 mm height (h_0) to samples, namely the given impact energy was 0.5 J. The dimensions of samples were length 45 mm, width 45 mm, and thickness 5 mm in total. The cured resin laminates consisted of two hard epoxy resin plates with the energy absorbable soft resin, which was the damping adhesive layer. Each thickness was 2 mm (hard resin)/2 mm (soft resin)/1 mm (hard resin). After the impact loading to the side of the 2 mm-thick hard resin plate of samples, the pendulum was rebounded from the sample to a height (h). Then, the energy absorbability E (%) was calculated by the next equation: $E = 100\{1 - (h/h_0)\}$.

RESULTS AND DISCUSSION

Viscoelastic properties of cured resins

The temperature dependencies of the viscoelastic properties (storage modulus: E' and loss tangent: tanδ) of CTBN/epoxy (CTBN/DGEBA/DDM) blend resins including 60 wt % CTBN and an unmodified epoxy resin (DGEBA/DDM) are shown in Figure 4. Three kinds of CTBN/epoxy resins indicated broad glass transition region from −50 to 50°C, which differed from unmodified resin with a sharp tanδ peak at 175°C. The resin including CTBN with AN 10 mol % had a relatively sharp first tanδ peak around −50°C and a broad second tanδ peak around 15°C. In the case of the resin including CTBN with AN 18 mol %, the second tanδ peak existed at almost the same temperature, but the first tanδ peak shifted to −35°C. Moreover, in the resin including CTBN with AN 26 mol %, the first tanδ peak shifted to a higher temperature and combined with the second broad peak. These data suggest that the AN mol % would be a key factor in controlling the compatibility between CTBN and epoxy, which was ascertained in the next section.

Morphologies of cured resins

Figure 5 shows overviews of the cured resins. The transparency of the resins was enhanced with the AN content in CTBN. To examine the internal morphologies of the cured resins, reflected electron images of SEM are shown in Figure 6. Thin sections of the resins were stained by OsO_4 before the observation. The OsO_4 stains rubber-rich regions, which were observed as bright areas in the reflected electron

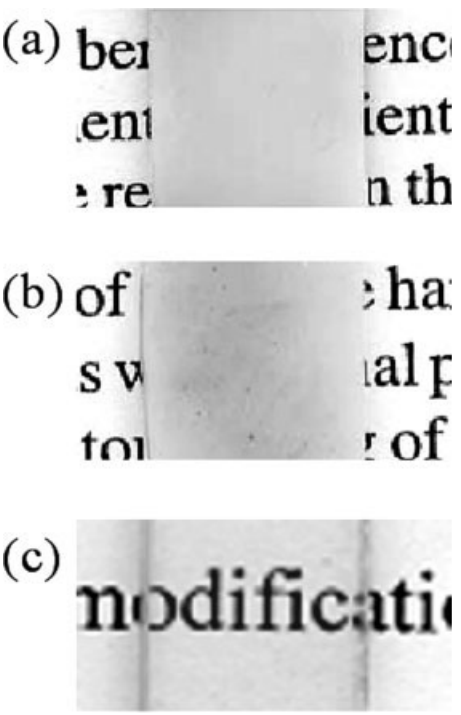

Figure 5 Overviews of CTBN/epoxy cured resins: (a) DGEBA/DDM/CTBN (100/14.4/172.4), AN content: 10 mol % in CTBN; (b) DGEBA/DDM/CTBN (100/14.4/172.4), AN content: 18 mol % in CTBN; (c) DGEBA/DDM/CTBN (100/14.4/172.4), AN content: 26 mol % in CTBN.

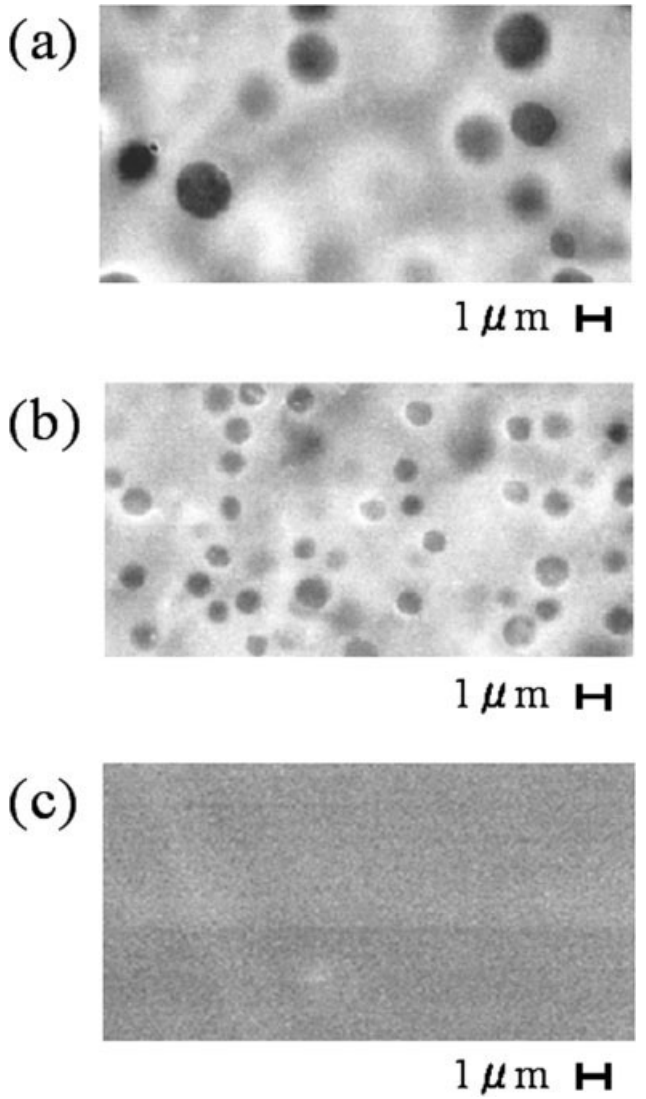

Figure 6 Morphologies of CTBN/epoxy polymer blends (reflected electron image of scanning electron microscopy after staining by OsO_4): (a) DGEBA/DDM/CTBN (100/14.4/172.4), AN content: 10 mol % in CTBN; (b) DGEBA/DDM/CTBN (100/14.4/172.4), AN content: 18 mol % in CTBN; (c) DGEBA/DDM/CTBN (100/14.4/172.4), AN content: 26 mol % in CTBN.

mode. The resin including CTBN with AN 10 mol % had the rubber-rich continuous phase, and epoxy-rich domains with 1–2 μm diameters. The resin including CTBN with AN 18 mol % also had similar phase structures, but the diameters of epoxy-rich domains were almost less than 1 μm. In *Viscoelastic properties of cured resins*, a sharp first tanδ peak was found around −50°C in the resins including CTBN with AN 10 mol %. This peak is attributable to CTBN-rich phases, and a broad tanδ peak is attributable to epoxy-rich phases with CTBN components. In the resins including CTBN with AN18 mol %, the first tanδ peak shifted to a higher temperature. This means the increased AN content in CTBN enhanced the compatibility between CTBN and epoxy. As the results, the rubber-rich phases included more epoxy components than the resin including CTBN with 10 mol %, and the diameters of epoxy-rich phases decreased.

It was interesting to note that no phase structures were observed from the resin including CTBN with AN 26 mol %, which means good compatibility among CTBN, DGEBA, and DDM was achieved in nano-scale. This should account for the alternation on the viscoelasticity of cured resins (Fig. 4) as described in *Viscoelastic properties of cured resins*. Although no phase separation was observed in the resin including CTBN with AN 26 mol %, some heterogeneity of internal structure in nano-scale would still exist in the resin, which resulted in the broad glass transition region.

Damping properties of steel laminates with the CTBN/epoxy resin layer

Figure 7 shows the loss factors of steel laminates adhered with formulated epoxy resins, as a function of the resonant frequencies. The steel laminates had several vibration modes. For example, laminates adhered with DGEBA/DDM exhibited the first resonance at 720 Hz, the second at 3680 Hz, and the third at 8390 Hz. In the laminates adhered with CTBN/epoxy including CTBN with AN 26 mol %, the first resonance occurred at 460 Hz, the second at 2110 Hz, and the third at 5190 Hz. The differences on the resonant frequencies among specimens are probably caused by the difference in stiffness of the resin layer of each specimen shown in Figure 4. Needless to say, the incorporation of CTBN decreased the stiffness of the epoxy resin. In a same resin composition, the stiffness of the resin enhanced

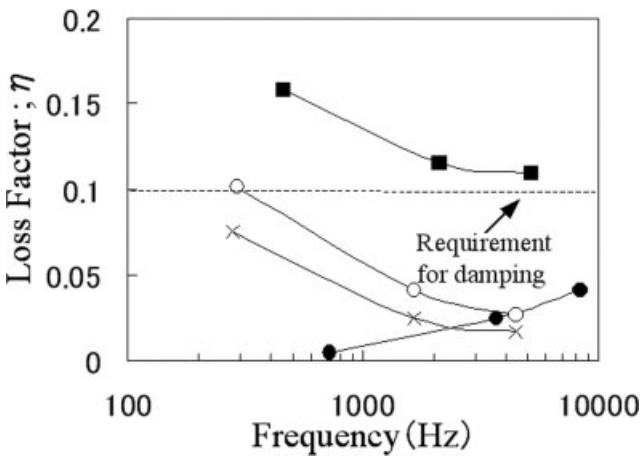

Figure 7 Loss factors of steel laminates adhered with formulated epoxy resins as constrained-layer, at 20°C on the several resonant points: ×, DGEBA/DDM/CTBN (100/14.4/172.4), AN content: 10 mol % in CTBN; (○), DGEBA/DDM/CTBN (100/14.4/172.4), AN content: 18 mol % in CTBN; (■), DGEBA/DDM/CTBN (100/14.4/172.4), AN content: 26 mol % in CTBN; (●), DGEBA/DDM (100/26.2).

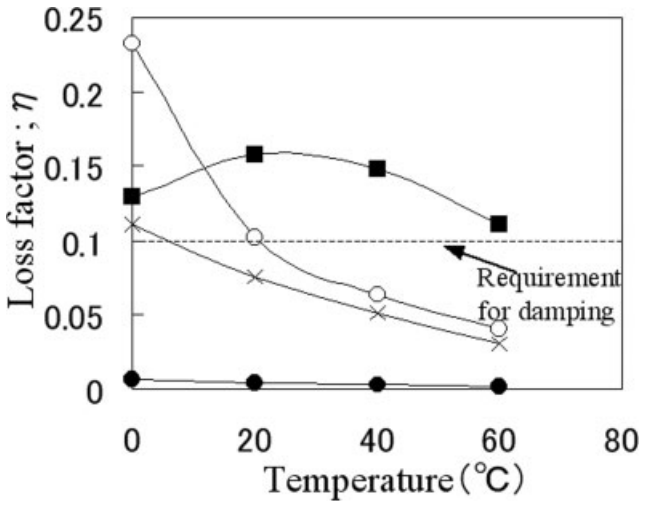

Figure 8 Temperature dependence of loss factors at the first resonant points of steel laminates adhered with formulated epoxy resins as constrained-layer: ×, DGEBA/DDM/CTBN (100/14.4/172.4), AN content: 10 mol % in CTBN; (○), DGEBA/DDM/CTBN (100/14.4/172.4), AN content: 18 mol % in CTBN; (■), DGEBA/DDM/CTBN (100/14.4/172.4), AN content: 26 mol % in CTBN; (●), DGEBA/DDM (100/26.2).

as increasing with the AN content in CTBN. Higher stiffness of the resin layer resulted in higher resonant frequencies of the specimens in the each vibration mode in Figure 7.

CTBN/epoxy blend resins had higher damping loss factors than the conventional hard epoxy resin (DGEBA/DDM). In particular, CTBN/epoxy including CTBN with AN 26 mol % indicated the highest loss factors among 4 steel laminates. The loss factors were over a requirement for damping ($\eta = 0.1$)[2,17,18] at several resonant frequencies.

Figure 8 shows the loss factors at the first resonant points of steel laminates as a function of the environmental temperatures. In this case also, CTBN/epoxy including CTBN with AN 26 mol % indicated the highest loss factors among four steel laminates in wide temperature range.

These damping properties can be explained by RUK method,[19] which calculates the loss factors (η) of a constrained laminates consisting of two steel plates with an intermediate viscoelastic resin layer, using the next equations.

$$\eta = \frac{(\tan\delta)XY}{1 + (2 + Y)X + (1 + Y)[1 + (\tan\delta)^2]X^2}$$

$$\frac{1}{Y} = \frac{E_1 {h_1}^3 + E_3 {h_3}^3}{12\mathrm{d}^2}\left(\frac{1}{E_1 h_1} + \frac{1}{E_3 h_3}\right)$$

$$X = \frac{G_2'}{p^2 h_2}\left(\frac{1}{E_1 h_1} + \frac{1}{E_3 h_3}\right)$$

The tanδ is the loss tangent of the viscoelastic resin layer, Y is the stiffness parameter of the laminates, and X is the shear parameter. E_1 and E_3 are the elastic moduli of the top and bottom steel layers, respectively; G_2' is the shear storage modulus of the viscoelastic resin layer; h_1, h_2, and h_3 are the thickness of the corresponding layers; d is the distance between the neutral planes of the two steel layers; and p is the wave number of the laminates at the resonant frequency. The tanδ and G_2' were determined by the DMA method in *Viscoelastic properties of cured resins*. The temperature dependencies of the calculated loss factors of the laminates are shown in Figure 9. The calculated loss factors are not exactly the same as the experimental results in Figure 8, but the rank order among the resins indicated good correspondence between them. This means that the viscoelasticity (both tanδ and shear modulus) of the adhesive resins determined the loss factors of the laminates.

Energy absorbability of resin laminates with the CTBN/epoxy resin layer

Next, the impact energy absorbability of these resins was examined. The resin laminates consisted of two hard epoxy resin (DGEBA/DDM) plates adhered with the energy absorbable CTBN/epoxy resin layer, which is the damping layer. The energy absorbability E (%) of the resin laminates was shown in Figure 10. The laminates adhered with CTBN/epoxy resin including CTBN with AN 26 mol % indicated higher energy absorbability than any other laminates. The rank order of the energy absorbability among the

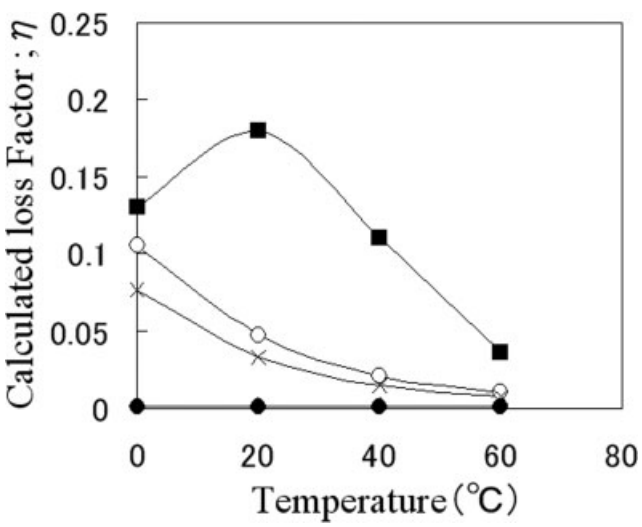

Figure 9 Calculated loss factors using RUK equation at the first resonant points of steel laminates, adhered with formulated epoxy resins as constrained-layer: ×, DGEBA/DDM/CTBN (100/14.4/172.4), AN content: 10 mol % in CTBN; (○), DGEBA/DDM/CTBN (100/14.4/172.4), AN content: 18 mol % in CTBN; (■), DGEBA/DDM/CTBN (100/14.4/172.4), AN content: 26 mol % in CTBN; (●), DGEBA/DDM (100/26.2).

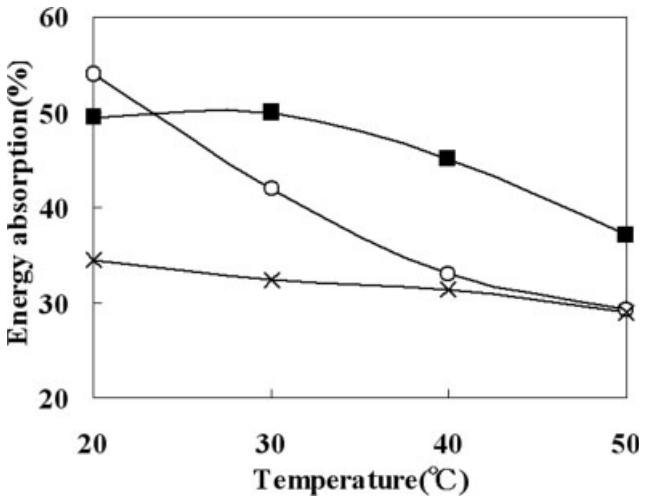

Figure 10 Energy absorbability of resin laminates with CTBN/epoxy resins as an adhesive layer: ×, DGEBA/DDM/CTBN (100/14.4/172.4), AN content: 10 mol % in CTBN; (○), DGEBA/DDM/CTBN (100/14.4/172.4), AN content: 18 mol % in CTBN; (■), DGEBA/DDM/CTBN (100/14.4/172.4), AN content: 26 mol % in CTBN.

resins in Figure 10 indicated good correspondence to that of the damping performance in Figure 8. Both energy absorbability and damping effect of the resins would originate in the molecular motion and the friction of polymer chains, by which the given mechanical energy would be converted into thermal energy and dissipated as heat release. The resin including CTBN with AN 26 mol % with the appropriate compatibility would have diverse relaxation mechanisms in the wide temperature range. The energy absorbability of the CTBN/epoxy bulk resin was also compared to other plastics and rubbers, such as poly (methyl methacrylate), polycarbonate,

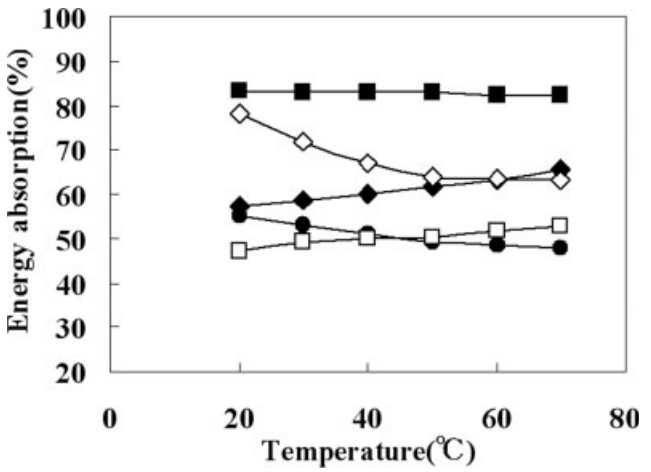

Figure 11 Energy absorbability of bulk resins: (■), DGEBA/DDM/CTBN (100/14.4/172.4), AN content: 26 mol % in CTBN; (◊), isoprene rubber; (♦), poly (methyl methacrylate); (□), polycarbonate; (●), DGEBA/DDM.

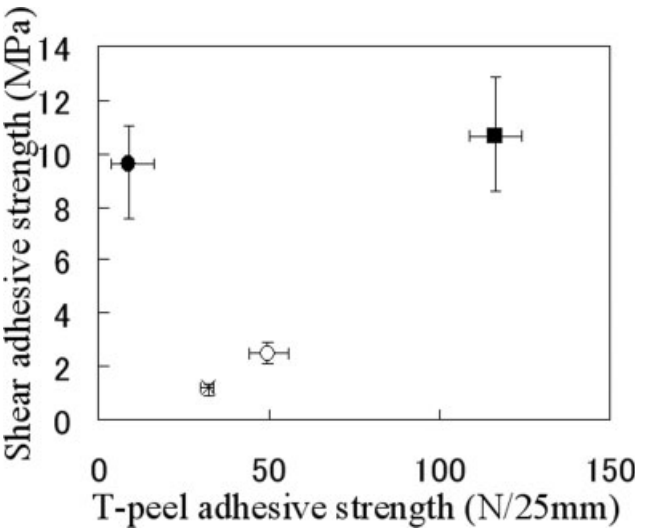

Figure 12 Shear adhesive strength and T-peel adhesive strength of epoxy resins: ×, DGEBA/DDM/CTBN (100/14.4/172.4), AN content: 10 mol % in CTBN; (○), DGEBA/DDM/CTBN (100/14.4/172.4), AN content: 18 mol % in CTBN; (■), DGEBA/DDM/CTBN (100/14.4/172.4), AN content: 26 mol % in CTBN; (●), DGEBA/DDM (100/26.2).

and isoprene rubber, as shown in Figure 11. The resin including CTBN with AN 26 mol % indicated higher energy absorbability than isoprene rubber in a wide temperature range from 20 to 70°C.

Adhesive properties of CTBN/epoxy resins

In addition, the adhesive properties of the resins were examined. Figure 12 shows both shear adhesive strength and T-peel adhesive strength of the resins. Conventional hard epoxy resin (DGEBA/DDM) had a high shear adhesive strength, but the T-peel adhesive strength was very low. All fracture modes of the specimens were interfacial failure. CTBN/epoxy resins including CTBN with AN 10~18 mol % indicated marginal T-peel adhesive strengths, but the shear adhesive strengths were very low. On the other hand, the resin including CTBN with AN 26 mol % indicated both high shear adhesive strength and high T-peel adhesive strength. In all the specimens of CTBN/epoxy resins, the fracture modes were cohesive failures in the adhesive resin layer. This implies that the adhesive strengths of these CTBN/epoxy resins were mainly determined by the mechanical properties of the bulk resins. Therefore, the tensile properties of the CTBN/epoxy bulk resins were examined, as shown in Figure 13. CTBN/epoxy resin including CTBN with AN 10 mol % indicated very low modulus of elasticity and tensile strength. The resin including CTBN with AN 18 mol % showed enhanced modulus, but the tensile strength was still less than 2 MPa. CTBN/epoxy resin includ-

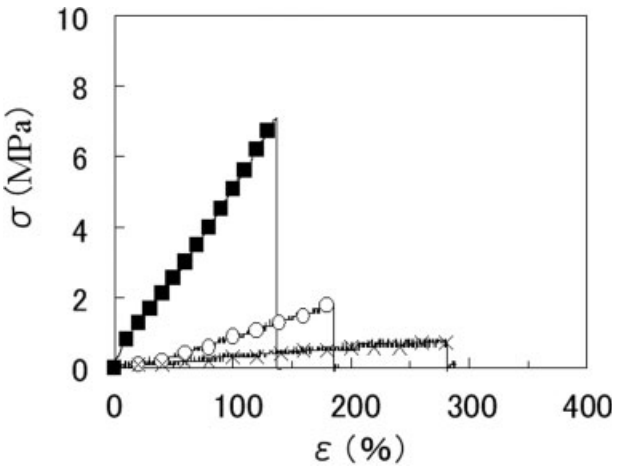

Figure 13 Tensile stress-strain behaviors of bulk epoxy resins: ×, DGEBA/DDM/CTBN (100/14.4/172.4), AN content: 10 mol % in CTBN; (○), DGEBA/DDM/CTBN (100/14.4/172.4), AN content: 18 mol % in CTBN; (■), DGEBA/DDM/CTBN (100/14.4/172.4), AN content: 26 mol % in CTBN.

ing CTBN with AN 26 mol % indicated the highest modulus of elasticity and the highest tensile strength of all. These data suggested that the strength and the fracture energy (strain energy to failure) of the bulk resins were reflected in the shear adhesive strength and the peel adhesive strength, respectively. The source of the high strength and the fracture energy of the bulk resin were the well-compatibilized cross-linked polymer networks, which were composed of CTBN, epoxy and DDM.

CONCLUSIONS

1. CTBN/epoxy polymer alloys, in which CTBN was the major component, were newly formulated. The cured resin including CTBN with AN 26 mol % did not show clear micro-phase separation, which means the components achieve good compatibility in nano-scale.
2. The polymer alloy resin with the adequate compatibility had broad glass-transition temperature range. This resulted in the high loss factor ($\eta > 0.1$) in broad temperature range and at several resonant frequencies of the steel laminates, which consisted of two steel plates with the resin layer in between.
3. The resin also indicated high adhesive strengths on aluminum substrates under both shear and peel stress mode. The high adhesive strengths of the CTBN/epoxy alloy originated in the high strength and the strain energy to failure of the bulk resin.

References

1. Technologies and laws for prevention of environmental pollutions (Vibration), Ministry of Economy, Trade and Industry in Japan, eds. Maruzen, Tokyo 2005.
2. Oborn, J.; Bertilsson, H.; Rigdahl, M. J Appl Polym Sci 2001, 80, 2865.
3. Corsaro, R. D.; Sperling, L. H. ACS Symposium Series 424; American Chem Society, Washington DC, 1990.
4. Sophiea, D.; Klempner, D.; Sendijarevic, V.; Suthar, B.; Frisch, K. C. Adv in Chemistry Series 239; Klempner, D.; Sperling, L. H.; Utracki, L. A. Eds., American Chemical Society: Washington DC 1994, pp 39–75.
5. Huelck, V.; Thomas, D. A.; Sperling, L. H. Macromolecules 1972, 5, 348.
6. Sperling, L. H.; Chiu, T. W.; Gramlich, R. G.; Thomas, D. A. J Paint Technol 1974, 46, 4.
7. Sperling, L. H. Comprehensive Polymer Science; Allen, G., Ed.; Pergamon Press: New York, 1989; Vol. 6, p. 423.
8. Frisch, K. C.; Klempner, D.; Frisch, H. L. Polym Eng Sci 1082, 22, 1143.
9. Xiao, H. X.; Frisch, K. C.; Frisch, H. L. J Polym Sci Polym Chem Ed 1982, 21, 2547.
10. Chang, M. C. O.; Thomas, D. A.; Sperling, L. H. J Polym Sci Polym Phys Ed 1988, 26, 1627.
11. Omoto, M.; Kusters, J.; Sophiea, D.; Klempner, D.; Frisch, K. C. Polym Mater Sci Eng 1988, 58, 459.
12. Yee, A. F.; Pearson, R. A. J Mater Sci 1986, 21, 2462.
13. Pearson, R. A.; Yee, A. F. J Mater Sci 1986, 21, 2475.
14. Kinloch, A. J.; Shaw, S. J.; Tod, D. A.; Hunston, D. L. Polymer 1983, 24, 1341.
15. Kishi, H.; Shi, Y.-B.; Huang, J.; Yee, A. F. J Mater Sci 1998, 33, 3479.
16. Young, R. J.; Lovell, P. A. Introduction to Polymers, Chapman & Hall: London, 1991; p. 420.
17. Liao, F.-S.; Hsu, T.-C. J.; Su, A. C. J Appl Polym Sci 1993, 48, 1801.
18. ASTM E756-83, Standard method for measuring vibration-damping properties of materials, American Society for Testing and Materials, Philadelphia, 1989.
19. Ross, D.; Ungar, E. E.; Kerwin, E. M. Structural Damping; ASME: Atlantic City, NJ, 1959; p 49.